Science Advances
AAAS

Supplementary Materials for

Many-body thermodynamics on quantum computers via partition function zeros

Akhil Francis, Daiwei Zhu, Cinthia Huerta Alderete, Sonika Johri, Xiao Xiao, James K. Freericks, Christopher Monroe, Norbert M. Linke, Alexander F. Kemper*

*Corresponding author. Email: akemper@ncsu.edu

Published 18 August 2021, *Sci. Adv.* **7**, eabf2447 (2021)
DOI: 10.1126/sciadv.abf2447

This PDF file includes:

Supplementary Materials for

I. DETAILED FORMALISM FOR LEE-YANG ZEROS

We consider an N site spin Hamiltonian $\mathcal{H}_s$ with an external field term $\mathcal{H}_B = h\sum_i \sigma_i^z$. Defining a variable $\tilde{z} = \exp(2\beta h)$, the partition function for N spins is written in terms of $\tilde{z}$

$$\begin{aligned}\mathcal{Z}(\beta, \mathcal{H}_s, h) &= \mathrm{Tr}[\exp(-\beta(\mathcal{H}_s + \mathcal{H}_B))] \\ &= \exp(-\beta N h)\sum_{k=0}^{N} p_k \tilde{z}^k \end{aligned} \tag{1}$$

where $p_k = \mathrm{Tr}_{\sum_i \langle\sigma_i^z\rangle = N-2k} \exp(-\beta\mathcal{H}_s)$ is the partition function in a zero magnetic field when k spins are in the $|\downarrow\rangle$ state. In order to get this expansion we have used the commutativity of $\mathcal{H}_s$ and $\mathcal{H}_B$. The partition function is expressed as an N^{th} order polynomial in terms of the variable $\tilde{z}$[1], which using the fundamental theorem of algebra we can rewrite in terms of its N zeros ($\tilde{z}_j$) as[2]

$$\mathcal{Z}(\beta, \mathcal{H}_s, h) = \exp(-\beta N h) p_N \ \Pi_{j=1}^{N} \left(\tilde{z} - \tilde{z}_j\right), \tag{2}$$

The coefficients of the polynomial are all positive numbers, thus its zeros cannot lie on the positive real axis of $\tilde{z}$(where the physical partition function exists), but must instead lie in the complex plane of h. Yet, if we can find the zeros, we may reconstruct the partition function from them.

Returning to the definition of the partition function, with the magnetic field as complex quantity $h = h_r + ih_i$:

$$\mathcal{Z}(\beta, \mathcal{H}_0, h_i) = \mathrm{Tr}\exp\left(-\beta\mathcal{H}_0 - i\beta h_i \sum_{j=1}^{n} \sigma_j^z\right) \tag{3}$$

where $\mathcal{H}_0 = \mathcal{H}_s + Re(\mathcal{H}_B)$. At this point, the imaginary part resembles a time evolution by a Hamiltonian $\sum_{i=1}^{n} \sigma_i^z$.

A measurable quantity $L(h)$, proportional to the complex partition function $\mathcal{Z}$ can be found as described in the main text.

$$L(h) = \frac{1}{\mathcal{Z}_0}\mathrm{Tr}\exp\left(-\beta\mathcal{H}_0 - i\beta h_i \sum_{i=1}^{n} \sigma_i^z\right), \tag{4}$$

where $\mathcal{Z}_0$ is the partition function $\mathrm{Tr}\, e^{-\beta\mathcal{H}_0}$. In order to achieve this, a probe or an ancilla qubit is attached to the system with the coupling Hamiltonian[24],

$$\mathcal{H}' = \frac{1}{2}\left(\sigma_{\mathrm{probe}}^z \otimes \sum_{i=1}^{n} \sigma_i^z\right). \tag{5}$$

The ancilla is initialised to be in the $|+\rangle$ state and the system in the thermal state, here $|+\rangle = \frac{1}{\sqrt{2}}[|0\rangle + |1\rangle]$. Thus the initial density matrix of the total system is

$$\rho(0) = \left(|+\rangle \langle +| \right) \otimes \frac{e^{-\beta \mathcal{H}_0}}{\mathcal{Z}_0}. \tag{6}$$

The "time-evolved" density matrix under the coupling Hamiltonian $\mathcal{H}'$ for a "duration" βh_i is,

$$\rho(\beta h_i) = e^{-i\mathcal{H}'\beta h_i} \rho(0) e^{i\mathcal{H}'\beta h_i}. \tag{7}$$

Since $\mathcal{H}_0$ commutes with $\mathcal{H}_B$, the density matrix becomes

$$\begin{aligned} \rho(\beta h_i) = & \frac{1}{2Z_0} \left(|\uparrow\rangle \langle\uparrow| e^{-\beta\mathcal{H}_0} + |\downarrow\rangle \langle\downarrow| e^{-\beta\mathcal{H}_0} \right) \\ & + \frac{1}{2Z_0} \left(|\uparrow\rangle \langle\downarrow| e^{-\beta\mathcal{H}_0} e^{-i\beta h_i \sum_{i=1}^{N} \sigma_i^z} + h.c. \right) \end{aligned} \tag{8}$$

Now $L(h)$ can be extracted from the off-diagonal terms of the reduced density matrix of the ancilla. The off-diagonal element of its density matrix (after tracing out the system) becomes

$$\rho_{\uparrow\downarrow}^{ancilla}(\beta h_i) = \frac{1}{2Z_0} \mathrm{Tr}_{\mathrm{sys}} \exp\left(-\beta\mathcal{H}_0 - i\beta h_i \sum_{i=1}^{N} \sigma_i^z \right) = \frac{1}{2} L(h) \tag{9}$$

Thus the real part of $L(h)$ can be extracted from the expectation value of σ_z of the ancilla after applying a Hadamard gate; similarly, the imaginary part of $L(h)$ can be extracted after applying an $R_x(-\pi/2)$ gate. Note that for this procedure, $\mathcal{H}_0$ needs to commute with $\mathcal{H}_B$. Otherwise, we need a different coupling Hamiltonian and the implementation becomes difficult[24].

The above described method can be summarised for the quantum simulation into the following three steps:

1. Prepare the system, including the probe, in its initial state according to Eq. 6.
2. Evolve with the Hamiltonian (Eq. 5), where the evolution operator is $U(\beta h_i) = \exp\left(-i\mathcal{H}'\beta h_i\right)$.
3. Measure the off-diagonal components of the ancilla density matrix to obtain $L(h)$. The zeros of $L(h)$ are the zeros of the partition function $\mathcal{Z}$

A. Lee-Yang Zeros for the Ising model

The one dimensional Ising Hamiltonian with periodic boundary condition for N sites is

$$\mathcal{H} = -J \sum_{i=1}^{N} \sigma_i^z \sigma_{i+1}^z - h \sum_{i=1}^{N} \sigma_i^z. \tag{10}$$

For the ferromagnetic case, where $J > 0$, the Lee-Yang zeros are purely imaginary in h and are given in terms of $\tilde{z} = \exp(-2\beta h)$ as

$$\tilde{z} = -e^{-4\beta J} \left(1 + \cos(k_n)\right) + \cos(k_n) \pm i\sqrt{\left(1 - e^{-4\beta J}\right) \left[\sin(k_n)^2 + e^{-4\beta J}(1 + \cos(k_n))^2\right]} \tag{11}$$

for $k_n = \frac{\pi(2n-1)}{N}$, where N is the number of sites and $n \in \{0, \ldots, N\}$. This result may be obtained from a transfer matrix formalism[17,25]. Since the zeros are purely imaginary in h, $\tilde{z} = \exp(-2\beta h)$ lies on the unit circle, as shown in Fig. S1. As the temperature is increased, the distribution of zeros collapses to a point where $2\beta h = \pi$. At lower temperatures, the zeros complete the circle, pinching the real axis at the critical temperature, corresponding to $\tilde{z}_{\mathrm{crit}} = e^{-2\beta_{\mathrm{crit}} h}$.

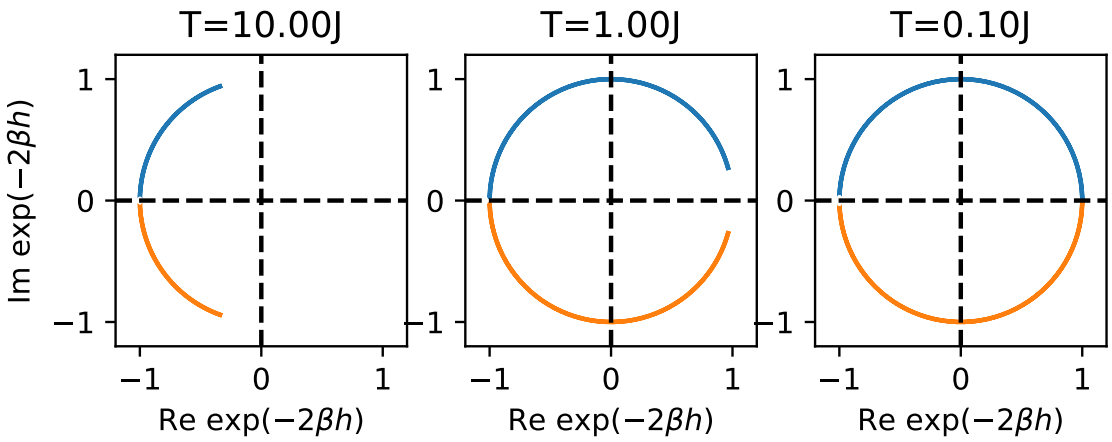

FIG. S1. Lee-Yang zeros for the classical Ising model.

B. Lee-Yang Zeros for the XY model

We next consider the XY model, where the Hamiltonian is

$$H = J\sum_i (\sigma_i^x \sigma_{i+1}^x + \sigma_i^y \sigma_{i+1}^y) + h\sum_{i=1}^{N} \sigma_i^z. \tag{12}$$

This model can be diagonalised through a Jordan-Wigner transformation followed by Fourier transformation. The Lee-Yang zeros in h are properly complex, with the imaginary part given by $\cos(2\beta h_i) = -1$ and the real part given by $h_r = -2J\cos(k)$, where k are the discrete quasi-momenta used in the Fourier-basis representation of the chain[5].

C. Lee-Yang Zeros for the two site XXZ model

The two site XXZ Hamiltonian is

$$H = J(\sigma_1^x \sigma_2^x + \sigma_1^y \sigma_2^y) + J_z(\sigma_1^z \sigma_2^z) + h(\sigma_1^z + \sigma_2^z). \tag{13}$$

Here, the Lee-Yang zeros occur at the values of h shown in Table S1. We note that if $h_1 = h_r + ih_i$ corresponds to a zero, then so does $-h_1$. Thus if $\tilde{z}_1 = \exp(2\beta h_1)$ is one solution to the polynomial, then the other solution is given by $\tilde{z}_2 = \exp(-2\beta h_1)$. We may also read off from the partition function that Ising-like zeros are found when $\cosh(2\beta J) < \exp(-2\beta J_z)$, and vice versa for XY-like zeros.

Type	h_r	h_i
Ising	$h_r = 0$	$\cos(2\beta h_i) = -\cosh(2\beta J)\exp(2\beta J_z)$
XY	$\cosh(2\beta h_r) = \cosh(2\beta J)\exp(2\beta J_z)$	$2\beta h_i = (2n+1)\pi$

TABLE S1. Real/imaginary parts of the complex magnetic field h where the zeros of the 2-site XXZ model occur.

II. CIRCUIT FOR THE PREPARATION OF THE TFD STATE OF THE 2-SITE XXZ MODEL

To find the location of the Lee-Yang zeros of a system with Hamiltonian H_A, we need to prepare a thermal density matrix at a particular temperature, $\rho_\beta = \mathcal{Z}^{-1} e^{-\beta H_A}$. This can be obtained by tracing out one subsystem from a

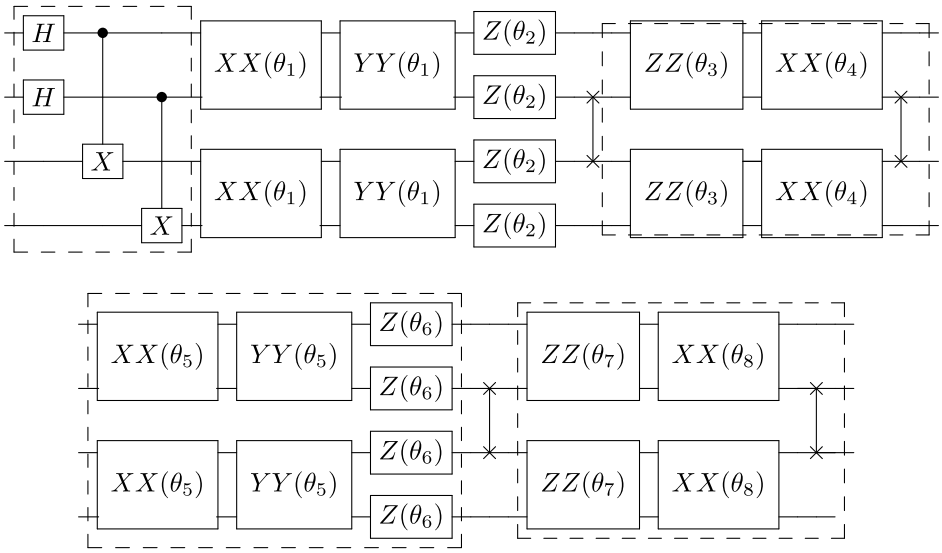

FIG. S2. Circuit to prepare a thermofield double state of the 2 site XXZ model with 8 parameters $\theta_1, \ldots \theta_8$. Here $XX(\theta) = \exp(-i\theta\sigma_x\sigma_x), YY(\theta) = \exp(-i\theta\sigma_y\sigma_y), ZZ(\theta) = \exp(-i\theta\sigma_z\sigma_z), Z(\theta) = \exp(-i\frac{\theta}{2}\sigma_z)$

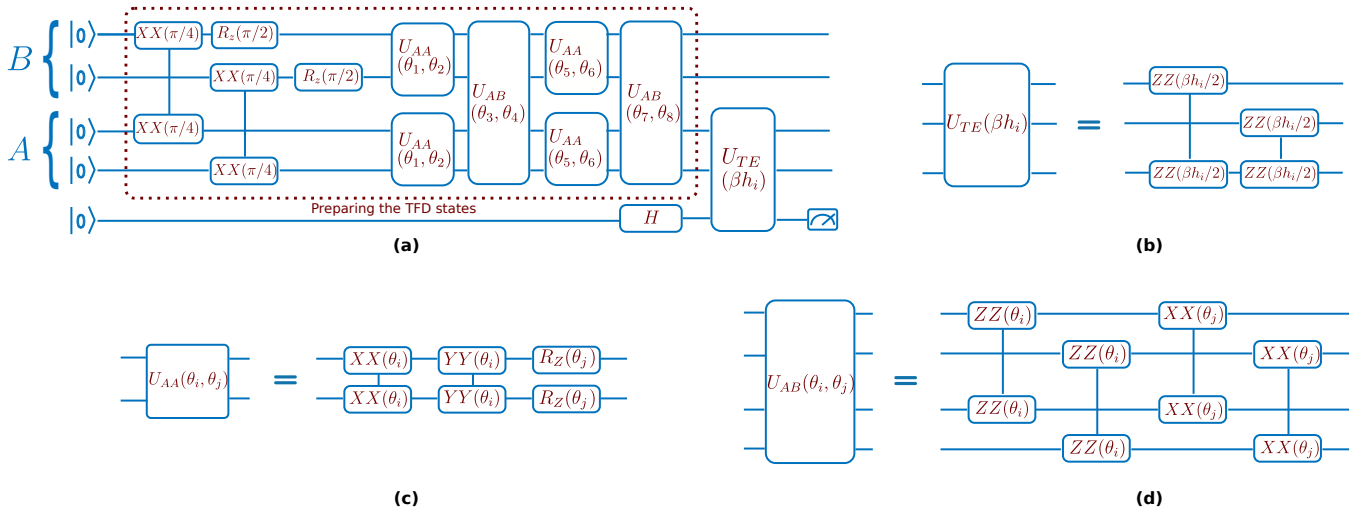

FIG. S3. Experimental realization of the full circuit. (a) Overview indicating the operative parts: TFD preparation via an alternating operator ansatz, followed by time evolution under the interaction Hamiltonian. (b)-(d) Decomposition of the time evolution and variational ansatz unitary operations into hardware native gates. Our native XX gate is defined as $XX(\theta) = e^{-i\sigma_x^{(j)}\sigma_x^{(k)}\theta}$, where j, k correspond to the two ions the gate is applied on. We convert this XX gate to YY and ZZ gates, defined as $YY(\theta) = e^{-i\sigma_y^{(j)}\sigma_y^{(k)}\theta}$ and $ZZ(\theta) = e^{-i\sigma_z^{(j)}\sigma_z^{(k)}\theta}$, respectively, by rotating the interaction axis through single qubit rotations. Here, $\sigma_\alpha^{(k)}$ is the α-th Pauli matrix applied to the k-th qubit.

TFD state which is defined in an expanded Hilbert space that contains two copies of the system:

$$|\,\mathrm{TFD}(\beta)\rangle = \frac{1}{\sqrt{Z}} \sum_n e^{-\beta E_n/2} |n\rangle_A |n\rangle_B, \tag{14}$$

where $H_A|n\rangle_A = E_n|n\rangle_A$. To prepare this TFD, a variational ansatz involving alternating evolution under Hamiltonians $H_A^{'}$, $H_B^{'}$, and H_{AB} is constructed[19,20] as shown in Fig. S2. $H_A^{'}$ and $H_B^{'}$ act identically on systems A and B respectively and are close in structure to the Hamiltonian H_A. H_{AB} is an inter-system Hamiltonian which entangles both systems. At the start, the system is prepared in a maximally entangled Bell state $\frac{1}{\sqrt{2}}(|00\rangle + |11\rangle)$, which is the ground state of H_{AB}. This ansatz starts from the correct thermal state for the sub system at infinite temperature

and when sufficient evolution layers are applied, can produce the thermal state at any temperature. In our case, $H_A^{'}$ was modified from H_A with an additional parameter in order to shorten the circuit depth.Thus the TFD ansatz has no ZZ part corresponding to H_A and Z gate has a different angle than XX, YY gates (see Fig. S2,S3).

The optimisation for the parameters was performed classically; the resulting circuit parameters θ_1 to θ_8 are given in the Table S2. Fig. S3 shows the hardware implementation of the final circuit.

J	$-\theta_1$	$-\theta_2/2$	$-\theta_3$	$-\theta_4$	$-\theta_5$	$-\theta_6/2$	$-\theta_7$	$-\theta_8$
0.9	0.409	0.785	0.480	1.660	0.395	0.785	0.739	1.178
0.96	1.178	0.392	0.555	1.427	1.092	0.392	0.694	-0.360
1.03	0.993	0.785	1.014	1.210	1.060	0.785	0.933	0.392
1.06	0.922	1.486	0.438	0.887	0.678	1.446	0.624	1.165
1.15	0.958	0.948	1.008	1.133	0.752	0.753	0.590	1.187
1.20	0.972	0.968	0.990	1.163	0.772	0.772	0.589	1.182

TABLE S2. Parameters θ_1 to θ_8 for the two site XXZ TFD preparation.

III. SIMULATION OF NOISE IN EXPERIMENT

On the ion trap quantum computer, the native two qubit gate used to implement entangling operations is ideally defined as $XX_{i,j}(t) = \exp(-it\sigma_i^x\sigma_j^x)$. In practice, the physical operation deviates from the ideal unitary. Previously the effect of random under or over rotations in the XX gate on the preparation of TFD states has been explored[20]. Here we study the effect of systematic shifts in the angle using a 'linear shift' error model which assumes a modified XX gate with two parameters a and b:

$$XX_{i,j}(t) \rightarrow [Z_i(bt_{trim}) \otimes Z_j(bt_{trim})] \cdot XX_{i,j}(at_{trim}) \cdot (\sigma^x \otimes \sigma^x)^n, \tag{15}$$

where $Z(\theta) = \exp(-i(\theta/2)\sigma^z)$. Here t_{trim} is the angle trimmed from t by adding or substracting $\pi/2$ n times so that the trimmed angle is in the range (-π/4,π/4). This is in accordance with how the XX gates are implemented on an ion-trap quantum computer. We performed a simulation in which all the XX gates in the circuit were replaced by this modified gate[51]. The optimised value of a and b are obtained by minimising the least square distance to data points and are given in Table S3. The corresponding plots are shown in Fig. S4. We see that the error is well modeled by the simulation.

J	a	b
0.9	0.99	-0.48
0.96	1.13	0.04
1.20	0.96	0.38

TABLE S3. Optimised values of the parameters for linear shift error model.

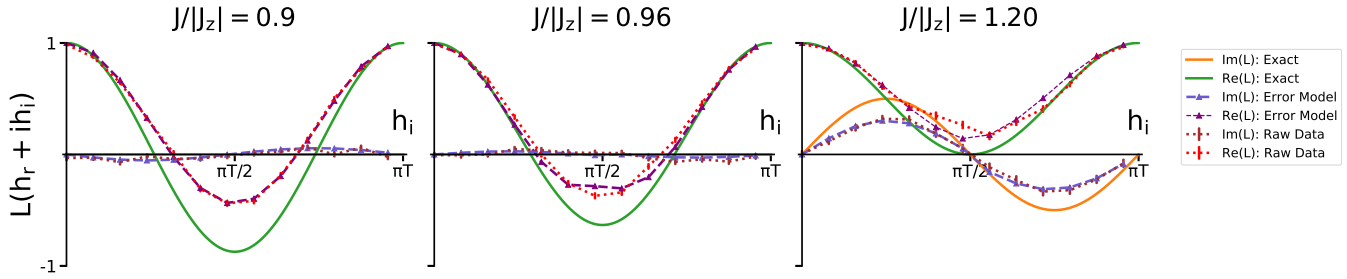

FIG. S4. L(h_i) obtained from the linear shift error model is compared with the actual data and exact values.

As we show below, the average value of the optimized error parameters is in line with the independently measured two-qubit gate error. The experimental two-qubit gate error is measured from counting populations in the computational basis. We can approximately derive the magnitude of this for our model by expanding in the XX error parameter as:

$$XX(at) = XX((1+\epsilon)t) \tag{16}$$
$$= \cos((1+\epsilon)t)I + i\sin((1+\epsilon)t)\sigma_x \otimes \sigma_x \tag{17}$$
$$\approx \left[\cos t - \epsilon t \sin t - \frac{\epsilon^2 t^2}{2}\cos(t)\right] I + i\left[\sin t + \epsilon t \cos t - \frac{\epsilon^2 t^2}{2}\sin t\right]\sigma_x\sigma_x + O\left(\epsilon^3\right) \tag{18}$$
$$= XX(t) + \epsilon t XX(\pi/2+t) - \frac{\epsilon^2 t^2}{2} XX(t) + O\left(\epsilon^3\right) \tag{19}$$

Therefore the error is proportional to ϵt. The maximum value of t is $\pi/4$. The average value of epsilon is measured to be 0.05 from the three data sets. Thus, the average error in the gate is $\sim \epsilon t$ is $0.06\pi/4 = 5\%$. This is close to the independently measured value of 2-3% for the 2-qubit gate error. The higher value measured from our fitting may signify the presence of additional sources of error such as cross talk.

Using the fidelity of the two qubit gates we could also estimate the maximum problem size that is within the reach of the current generation of hardware. Suppose we need the accuracy of the circuit to be at least 90% of the exact value. Then, if f is the fidelity of the two-qubit gates, and N_{2q} is the number of two qubit gates, we need $f^{N_{2q}} > 0.9$ The latest generation of trapped ion systems are at 99.9% two-qubit gate fidelity. In our circuit design, the time evolution for an n site model requires n two-qubit gates. For the preparation of the TFD, n two-qubit gates are required to make the initial Bell state, and let us assume that αn layers of the QAOA protocol are needed. In each layer there are $6n$ two-qubit gates. In total

$$N_{2q} = n + 6\alpha n^2 + n = 6\alpha n^2 + 2n$$

Thus,

$$f^{N_{24}} = f^{6\alpha n^2 + 2n} > 0.9$$

$$n < \frac{-1 + \sqrt{1 + 6\alpha \log_{0.999}(0.9)}}{6\alpha}$$

IV. POST-SELECTING EXPERIMENTAL DATA

Two post-selection schemes can be applied at the end of the circuit for calculating Lee-Yang zeros after preparing the TFD state corresponding to the XXZ model.

Method 1: For the XXZ model, the total magnetization $\sum_i \sigma_i^z$ is a good quantum number. Therefore, in the TFD state for this model,

$$|\Psi\rangle = \frac{1}{Z_\beta}\sum_j e^{-\beta E_j/2}\,|\phi_j\rangle_A\,|\phi_j\rangle_B\,, \tag{20}$$

we have $\sum_i \sigma_{i,A}^z = \sum_i \sigma_{i,B}^z$. Any runs of the circuit resulting in measurements that do not satisfy this condition can be discarded.

Method 2: Measuring the real part of the L(h) curves involves putting the ancilla qubit in the $(|0\rangle + |1\rangle)/\sqrt{2}$ state, followed by the operation $\exp\left(-i\frac{\theta}{2}\sigma_a^z \sum_i \sigma_i^z\right)$, where σ_a^z acts on the ancilla qubit and the sum is over the qubits in subsystem A of the TFD state, and an $R_y(-\pi/2)$ on the ancilla before measurement. For the 2-site XXZ model, this can be decomposed as in Fig. S5. Now, if $\sum_i \sigma_{i,A}^z = 0$, that is, $\sigma_{a_1}^z \neq \sigma_{a_2}^z$, the controlled rotations will cancel each other resulting in no phase generated on the ancilla qubit. After the final $R_y(-\pi/2)$, the ancilla qubit will then return to 0 with probability 1. Therefore, any runs of the circuit that result in a measurement in which the ancilla qubit is 1 but $\sigma_{a_1}^z \neq \sigma_{a_2}^z$ should be discarded.

Fig. S6 shows the effect of the two post-selection schemes on the measured data. As is clear from the figure, each method has a comparable (but minor) effect. In the main text, we have opted to use Method 1.

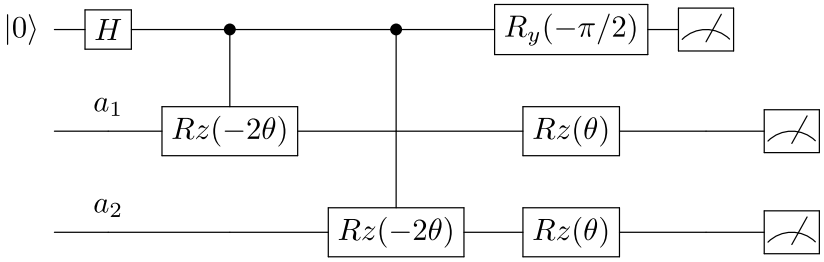

FIG. S5. Decomposition of the time evolution for post-selecting data.

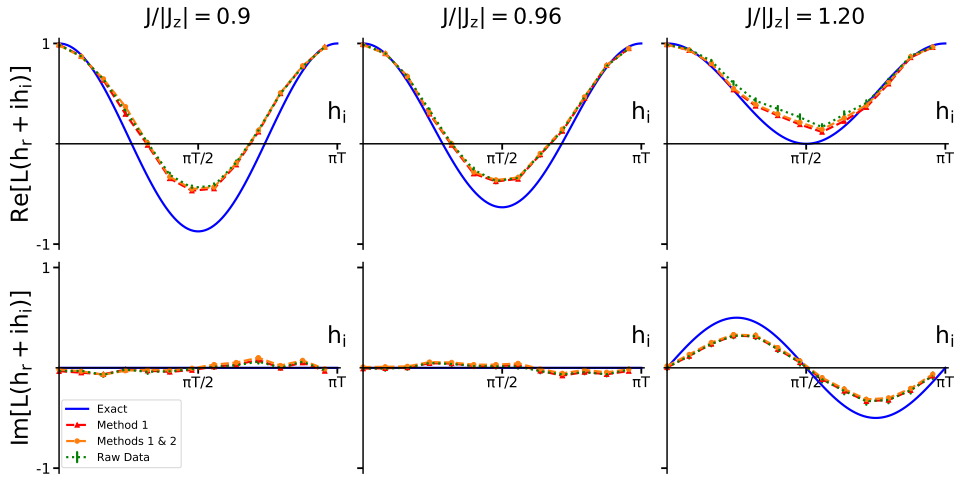

FIG. S6. Comparing different methods of data post selection demonstrates that neither method significantly improve the accuracy of the experimental data.

V. FISHER ZEROS

Following the study of Lee-Yang zeros, Fisher looked into the partition function zeros in terms of complex temperature [3]. While for the generic XXZ model analytical expressions are not known, they can be obtained for the two limiting cases — the Ising and XY model models. For the Ising model with Hamiltonian,

$$H = J\sum_{i}^{N}\sigma_i^z\sigma_{i+1}^z, \tag{21}$$

Fisher zeros are found at [12]

$$\beta = -\frac{1}{4J}\ln\tan^2\left[\frac{\pi}{N}(k+1/2)\right] \pm i\frac{\pi}{4J}(2m+1) \tag{22}$$

where $k = \{0, 1, ..., N-1\}$ and m is any integer. For the XY model diagonalisation is performed after mapping into a fermionic space using a Jordan-Wigner transformation. In order to compare Fisher zeros to the analytical expression we have considered the XY model with the boundary term which does not have any Jordan Wigner string.

$$H = J\sum_{i}^{N-1}(\sigma_i^x\sigma_{i+1}^x + \sigma_i^y\sigma_{i+1}^y) + H_b \tag{23}$$

H_b is the boundary term $H_b = 2J[\sigma_+^1\sigma_z....\sigma_z\sigma_-^N + \sigma_-^1\sigma_z....\sigma_z\sigma_+^N]$, where $\sigma_\pm = (\sigma_x \pm i\sigma_y)/2$. This gives the fermionic energies to be $4J\cos(\frac{2\pi}{N}k)$ where $k = \{0, 1, ..., N-1\}$. Hence, the Fisher zeros are found to be on the imaginary axis at

$$\beta = -i\frac{(2m+1)\pi}{4J\cos(\frac{2\pi}{N}k)} \tag{24}$$

where m is an integer.

The approach introduced in this work can be equally applied to finding Fisher zeros. In this case, the interaction Hamiltonian for the "time evolution" portion of the circuit is simply

$$\mathcal{H}' = \frac{1}{2}\left(\sigma^z_{anc} \otimes \mathcal{H}_0\right), \tag{25}$$

and this amounts to the application of a controlled unitary. When $\mathcal{H}_0$ is simple, this may be implemented without approximation, but for larger or more complex systems a Trotter decomposition of $\exp(-i\mathcal{H}_0\beta_i)$ may be necessary.

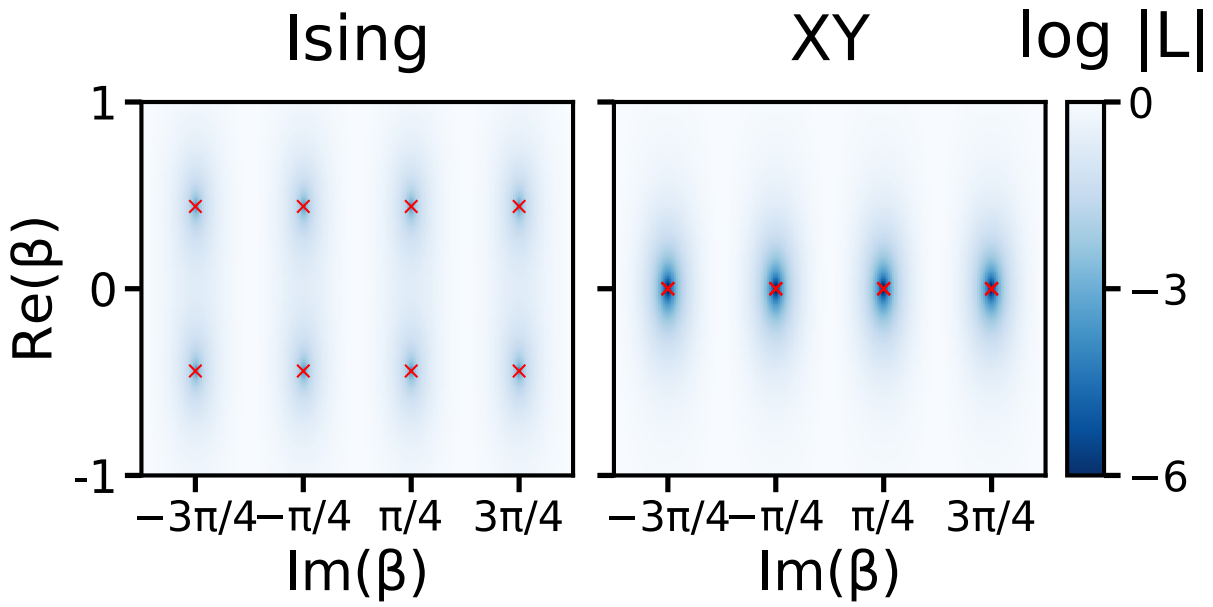

FIG. S7. Fisher zeros for the two limiting cases of a 4-site XXZ model.

For the two limiting cases under consideration—the XY model and the Ising model— the Fisher zeros also show a qualitative transition. Fig. S7 shows the location of the zeros for the two limits. The Ising model Fisher zeros lie parallel to the real axis[12] (similar to the XY Lee-Yang zeros), and the XY model Fisher zeros lie directly on the imaginary axis. In between, the features are more complex than the Lee-Yang zeros are, and depend heavily on the choice of boundary conditions; here we have chosen the boundary conditions that make the system amenable to a Jordan-Wigner transformation.